

Proteomic approach to enhance doxorubicin production in *panK*-integrated *Streptomyces peucetius* ATCC 27952

Eunjung Song · Sailesh Malla · Yung-Hun Yang ·
Kwangwon Lee · Eun-Jung Kim · Hei Chan Lee ·
Jae Kyung Sohng · Min-Kyu Oh · Byung-Gee Kim

Received: 13 August 2010/Accepted: 4 November 2010/Published online: 10 February 2011
© Society for Industrial Microbiology 2011

Abstract Biosynthesis of polyketide compounds depends upon the starter and extender units of coenzyme A derivatives of carboxylic acids present in the host organism. To increase the coenzyme A (CoA) pool, pantothenate kinase (*panK*) gene from *Escherichia coli* was integrated into *S. peucetius* ATCC 27952 (*panK*-integrated strain, BG200), which resulted in increase in aglycone polyketide ε -rhodomycinone (RHO), but decrease in the desired product, i.e., doxorubicin (DXR). To reduce RHO accumulation by synthesizing daunorubicin (DNR) from RHO more efficiently, glycosyltransferase (*dnrQS*) was overexpressed (pIBR25::*dnrQS* in *panK*-integrated strain, BG201). However, *DnrQS* overexpression still resulted in less production of DXR compared with the parental strain. To understand the results in detail by investigating the proteome changes in the *panK*-integrated strain, two-dimensional (2D) gel electrophoresis was performed. Among the several proteins that are up- or downregulated in BG200, efflux protein DrrA was our main target of

interest, because it is directly related to DXR/DNR production in *S. peucetius*. DXR transporter DrrAB was additionally introduced in BG200 to enhance secretion of toxic DXR. Compared with *S. peucetius* ATCC 27952, BG204 (pIBR25::*drrAB* in *panK*-integrated strain), produced two times higher amount of DXR, which is 9.4-fold higher than that of *panK*-integrated strain BG200. The results show that the proteomic approach is quite useful in host development of *Streptomyces* and understanding cell physiology for antibiotic production.

Keywords *Streptomyces peucetius* · 2-DE · nLC-MS/MS · Pantothenate kinase

Introduction

Recent advances in proteomic tools have made it possible to identify protein spots showing significant changes in cell expression levels directly in 2D gel under certain conditions [25]. Although DNA chip or ChIP-on-chip is the current standard protocol to understand global changes in the cell, 2D gel and subsequent mass spectrometry analyses have become complementary tools to confirm changes in protein levels in cells, especially when posttranslational modification becomes an issue in eukaryotic cell systems [13]. Although several groups have attempted to understand metabolic and physiological changes using proteomic tools, these approaches have not been widely used for actual engineering of target genes of secondary metabolites to enhance antibiotic production in *Streptomyces* species.

Since industrially useful polyketide antibiotics and fatty acids are mainly synthesized from CoA derivatives [14], overproduction of CoA is a prerequisite for mass production of those compounds. Pantothenate kinase (PanK),

E. Song · S. Malla · K. Lee · E.-J. Kim · B.-G. Kim (✉)
School of Chemical and Biological Engineering,
Institute of Molecular Biology and Genetics, and Bioengineering
Institute, Seoul National University, Seoul, Korea
e-mail: byungkim@snu.ac.kr

Y.-H. Yang
Department of Microbial Engineering, College of Engineering,
Konkuk University, Seoul, Korea

H. C. Lee · J. K. Sohng
Institute of Biomolecule Reconstruction (iBR),
Department of Pharmaceutical Engineering,
Sun Moon University, Asan, Korea

M.-K. Oh
Department of Chemical and Biological Engineering,
College of Engineering, Korea University, Seoul, Korea

which phosphorylates pantothenate, is known to be the most important key regulatory enzyme in the CoA biosynthetic pathway [8, 24]. Many studies have focused on increasing intracellular CoA levels via overexpressing pantothenate kinase to enhance production of industrially useful compounds derived from CoA or its thioesters in *E. coli* [21–23]. Since the effect of *panK* from *E. coli* on CoA pool increase is already well characterized [21–23], we wanted to analyze how this PanK affects CoA pools in *Streptomyces* strains, which produce various polyketide antibiotics using acyl-CoA intermediates. As a model system, doxorubicin (DXR) production was evaluated by chromosomal integration of *E. coli panK* into the *S. peucetius* genome.

Doxorubicin (DXR) is a clinically important type II polyketide-based anthracycline anticancer agent and is synthesized from one propionyl-CoA starter unit and nine malonyl-CoA extender units in *Streptomyces peucetius* ATCC 27952. In the DXR biosynthetic pathway, these starter and extender units are used to form aklanonic acid, which is further converted to a polyketide-derived aglycone, ϵ -rhodomycinone (RHO). Then thymidine diphosphate (TDP)-daunosamine, a deoxyhexose glycone unit, is attached to produce rhodomycin D in presence of the glycosyltransferase DnrS along with DnrQ, an auxiliary protein for glycosylation. Rhodomycin D is then converted to daunorubicin (DNR) via some additional steps, which is then hydroxylated to produce DXR by the action of cytochrome P450 enzyme DoxA [7]. Interestingly, *panK*-integrated strain enhanced aglycone production (RHO), but the product of our interest, i.e., DXR, was less produced. To understand the metabolic network changes and find strategies to improve DXR production in *panK*-integrated strain, proteomic expression levels were analyzed by two-dimensional gel electrophoresis (2D gel) followed by nLC-MS/MS. Our data showed that *panK* integration alone could not increase DXR/DNR biosynthesis but enhanced the yield when coupled with efflux protein overexpression, suggesting that complex and tight regulation of cellular processes plays a significant role in DXR production in *S. peucetius*.

Materials and methods

Bacterial strains, plasmids, and culture conditions

E. coli strains were cultured in Luria–Bertani (LB) medium at 37°C. *E. coli* XL1-Blue (Stratagene) and *E. coli* JM110 (Promega) hosts were used for DNA manipulation and demethylation of plasmid DNA for transformation into *S. peucetius*, respectively. *S. peucetius* ATCC 27952 was cultured at 30°C in R2YE medium [10] with 0.5% glycine for

preparation of protoplast, and NDYE medium [1] for DXR production. pGEM-T Easy (Promega, USA) was used as a cloning vector, whereas pSET152 [4] and pIBR25 [20] were used as integration and expression vector, respectively. Ampicillin (100 µg ml⁻¹) and apramycin (100 µg ml⁻¹) were used for plasmid selection in *E. coli*.

Construction of recombinant plasmids

A set of primer pairs, 5'-ATAT GGATCC AGC AAC GGA GGT ACG GAC ATG AGT ATA AAA GAG CAA ACG-3' and 5'-ATAT TCTAGA TTA TTT GCG TAG TCT GAC CTC-3', were synthesized with *Bam*HI and *Xba*I sites (restriction sites underlined), respectively, and were used for amplification of nucleotide sequences of *panK* (951 bp) from the chromosomal DNA of *E. coli* strain. The polymerase chain reaction (PCR) product was cloned into pSET152 at the *Bam*HI/*Xba*I sites to construct pDK1609 integration recombinant plasmid. For overexpression of *dnrQS* and *drrAB* genes, recombinant expression plasmids pDnrQS25 and pDrrAB25 were constructed by Malla et al. [11, 12], respectively. The PCR products were cloned into pGEM-T Easy and sequenced prior to cloning into the integration vector to verify that no mutation had occurred during PCR amplification.

Generation of *panK*-integrated *S. peucetius* BG200 and overexpression of *dnrQS* or *drrAB* into BG200

The demethylated pDK1609 integration plasmids were introduced into *S. peucetius* by polyethylene glycol (PEG)-mediated protoplast transformation. The conditions for protoplast formation, regeneration, and DNA transformation were as we described previously [11]. To select *S. peucetius* transformants harboring pDK1609, 60 µg ml⁻¹ apramycin was applied. The transformants were regenerated up to fourth generation using apramycin antibiotics at 30°C, which resulted in the *panK*-integrated *S. peucetius* strain *S. peucetius* BG200. Integration of *panK* into chromosomal DNA of *S. peucetius* was confirmed by PCR using the primer pair 5'-CAA TAC GAA TGG CGA AAA GCC GAG CT-3' and 5'-CCT CTG GCG GAT GCA GGA AGA TCA A-3' designed from apramycin [*aac(3)IV*] gene. For overexpression of *dnrQS* or *drrAB*, the demethylated recombinant expression plasmids pDnrQS25 and pDrrAB25 were transformed into BG200 by using PEG-mediated protoplast transformation as mentioned above. Thus generated recombinant strains *S. peucetius* BG201 (pIBR25::*dnrQS* in *panK*-integrated strain) and BG204 (pIBR25::*drrAB* in *panK*-integrated strain) were screened by using 15 µg ml⁻¹ thiostrepton and 60 µg ml⁻¹ apramycin.

Isolation of secondary metabolites using HPLC analysis and metabolite identification using ESI-MS

For DXR, DNR, and RHO quantification, 500 μ L culture broth was extracted with equal volume of isopropyl alcohol-HCl (49:1, v:v) at 30°C, 200 rpm for 30 min. The extract was filtered and analyzed by high-performance liquid chromatography (HPLC) using a Waters Symmetric C18 column (250 \times 4.6 mm, 5 μ m particle size) with mobile phase of 50% acetonitrile in water containing 0.068% phosphoric acid and 0.1% sodium dodecyl sulfate (SDS) with flow rate of 1 ml min⁻¹ and HPLC diode array detector set at 495 nm [15]. Standard calibration curves were used for concentration determination using peak area.

The collected fraction was analyzed with Thermo Scientific LCQ DecaXP ESI mass spectrometer with 50% acetonitrile in 0.1% formic acid as mobile phase of the microLC system. The fraction of major peak at retention time of 11.2 min (Fig. 1) was determined to be RHO in both negative and positive ionization mode. The MS/MS fragment pattern was also analyzed, being in agreement with that reported for authentic compound [16].

Malonyl-CoA quantification

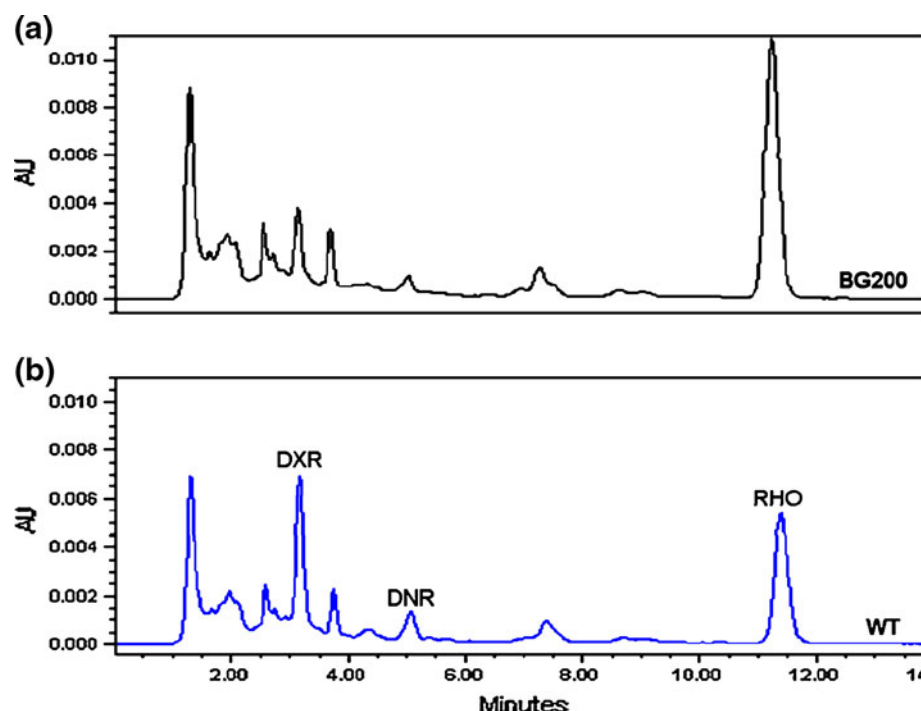
Malonyl-CoA was extracted as previously reported with some modification [18]. *S. peucetius* ATCC 27952 and BG200 were cultured in NDYE liquid media, and 3 ml culture broth was taken each day from day 1 to 4. The

collected samples were centrifuged at 4°C at 13,200 rpm for 5 min; cells were disrupted with 300 μ L 15% trichloroacetic acid (TCA) solution and centrifuged again for 5 min. The supernatant was passed through an OASIS HLB SPE cartridge under vacuum as follows: The cartridge was first conditioned with methanol followed by 0.15% TCA solution. The extracts were then applied to the cartridge, followed by addition of 0.15% TCA solution as a wash step. The bound CoA-esters were eluted two times with 0.5 ml 5% NH₄OH in methanol, and evaporated to dryness using vacuum centrifuge and kept in a freezer until analysis. They were dissolved in 100 μ L water and analyzed by Thermo Scientific LCQ DecaXP ESI mass spectrometer. Hexanoyl-CoA was used as an internal standard to normalize the peak area of malonyl-CoA standard and the real samples. Quantification was done in selected ion monitoring (SIM) mode in positive mode using the two center mass ions: 855 ([M + H]⁺ of malonyl-CoA) and 867 ([M + H]⁺ of hexanoyl-CoA). Malonyl-CoA area calculated from the selected ion peak profiles was divided by the peak area arising from the internal standard. Malonyl-CoA concentration was calculated from the standard curve obtained from standard malonyl-CoA samples.

Two-dimensional gel electrophoresis

The mycelial broths were harvested at 60 h of growth, and the cell pellets were disrupted by sonication. Concentration of the obtained cytosolic protein was determined using the

Fig. 1 **a** HPLC data comparison between extracts of BG200 (*panK*-integrated *S. peucetius*) and **b** *S. peucetius* ATCC 27952; doxorubicin (DXR), daunorubicin (DNR), and ϵ -rhodomycinone (RHO) peaks are shown at retention times of 3.2, 5.1, and 11.2 min, respectively



Bradford assay (Bio-Rad). Protein extracts (80 µg) were mixed with 350 µL rehydration solution containing 8 M urea, 2% 3-[*(3-cholamidopropyl)dimethylammonio*]-1-propanesulfonate (CHAPS), 50 mM dithiothreitol (DTT), and 0.5% pH 4–7 Ampholine, and isoelectrically focused as the first dimensional separation using 18-cm IPG strips with linear pH gradient from 4 to 7 (GE Healthcare). Isoelectric focusing was carried out to a total of 87,000 Vh with maximum voltage of 5,000 V, followed by equilibration of the strips. The first equilibration was carried out in an equilibration solution containing 6 M urea, 2% SDS, 50 mM Tris-HCl, 30% glycerol, trace bromophenol blue, and 65 mM DTT (pH 8.8), and the second equilibration was carried out in the same equilibration solution with 135 mM iodoacetamide in place of 65 mM DTT, each for 15 min.

Second dimensional separation was performed using 12.5% polyacrylamide gels. To minimize experimental variation, two gels were run for each strain. Silver-stained gel images were then scanned with a POWERLook 1,100 densitometer (UMAX), and were analyzed by ImageMaster™ 2D Platinum software (GE Healthcare). Normalized percentage integrated optical density (% volume) was calculated for each of the protein spots detected.

Protein identification by nLC-MS/MS

Selected spots were excised from the gels with the tip of a clean polypropylene micropipette, and then each gel piece was digested by trypsin (Promega) for analysis by nLC-MS/MS (LCQ DecaXP ESI Mass Spectrometer, Thermo Scientific). A fused silica capillary column (360 µm OD, 100 µm ID) was pulled with a P-2,000 laser puller (Shutter Instrument) to create a nanospray tip. For liquid chromatography, pulled capillary columns (360 µm OD, 100 µm ID, 12 cm long) were packed with POROS R2 hydrophobic resin under nitrogen gas pressure. Tryptic peptides were then loaded onto a C18 packed tip and were separated using acetonitrile gradient at flow rate of 300 nL/min and introduced into the mass spectrometer with a nanospray source online in positive-ion mode. Spray voltage was 1.75 kV, and the heated capillary was maintained at temperature of 200°C. Peptide ions were detected in full-scan mode, followed by three data-dependent MS/MS scans. For analysis of MSⁿ fragmentation, 35–37% normalized collision energy and 1.5 Da isolation width were used. Most of the proteins were identified unambiguously because peptides with cross-correlation scores, XCorr, were equal or greater than 1.6 for singly charged, 2.2 for doubly charged, and 3.0 for triply charged peptides when searched with local *S. peuetius* database using TurboSEQUEST (Thermo Scientific).

Results and discussion

Generation of *S. peuetius* BG200 and secondary metabolite analysis

To assess the effect of chromosomal integration of *E. coli panK* on DXR production, the recombinant plasmid pDK1609 (pSET152: *panK*) was constructed. After transformation of pDK1609, the recombinant *S. peuetius* strains were grown with apramycin antibiotics (60 µg ml⁻¹) up to fourth generation. Chromosomal integration of *panK* was confirmed by PCR of an *acc(3)IV*-resistant marker, located in the pSET152 vector, from the genomic DNA of the selected strains. DXR, DNR, and RHO production of the integrated strain was measured. Then, intracellular malonyl-CoA level was measured to verify that the integration of *panK* was effectively functional to increase the CoA pool in *S. peuetius*. It was observed that the malonyl-CoA concentration of BG200 was 1.7-fold higher than that of wild type (WT) (Fig. 2).

When the extracts from *S. peuetius* wild type and BG200 were compared by HPLC, a prominent peak (Fig. 1) was detected (approximately twofold increase compared with the wild type), and the peak was collected and analyzed by ESI-MS (data not shown). The peak was confirmed to be RHO with *m/z* 427.02, which corresponds to [M - H]⁻ peak in negative mode, and *m/z* 450.80, which was a [M + Na]⁺ peak in positive mode. By integrating the *E. coli* pantothenate kinase gene into *S. peuetius* ATCC 27952, increased CoA pool led to twofold enhanced production of RHO, suggesting that the increased CoA pool was efficiently channeled to synthesize RHO, one of the anthracycline derivatives. However, DNR production did not change accordingly, and DXR production was rather decreased compared with that of *S. peuetius* ATCC

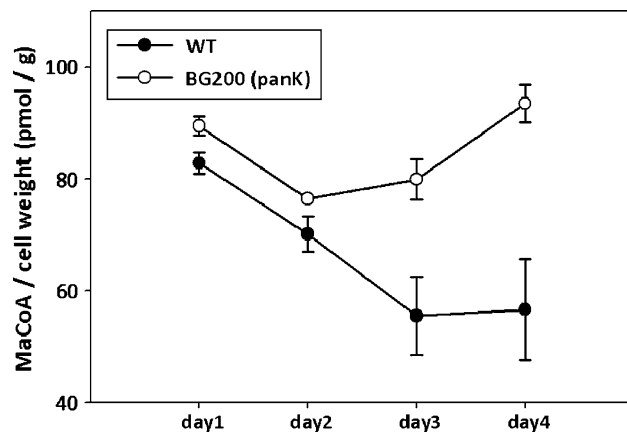


Fig. 2 a Time course of intracellular malonyl-CoA level measured by mass spectrometric method in WT *S. peuetius* ATCC 27952 (filled circles) and *panK*-integrated *S. peuetius* (BG200) (open circles) cultured in NDYE media for 96 h

27952, suggesting that TDP-daunosamine synthesis or glycosyltransferase activity (DnrQS) might be the rate-limiting step for DXR synthesis in BG200 [1]. To increase DXR production, firstly we attempted to increase glycosylation efficiency by overexpressing glycosyltransferase and its helper gene.

Effect of *dnrQS*-overexpressed *panK*-integrated *S. peucetius* (BG201) on DXR production

In DXR biosynthesis, DnrS catalyzes glycosylation of TDP-daunosamine to an aglycone RHO to form rhodomycin D, and DnrQ encodes a protein that is essential for the glycosylation [17]. To increase production of glycosylated DNR and DXR, DnrQS was overexpressed in *panK*-integrated *S. peucetius* (BG201), and the metabolites were quantified by HPLC (Fig. 3). Strain BG201 produced almost the same amount of DNR as BG200 and WT. Although BG201 produced threefold more DXR compared with BG200, its level was still lower compared with WT (0.6-fold).

Therefore, we reached the conclusion that the bottleneck in DXR/DNR production in RHO-overproducing BG200 was neither glycosylation nor glycone biosynthesis efficiency. To understand the global changes in BG200 and investigate why DXR production was decreased in the *panK*-integrated strain, comparative 2D gel analysis was performed.

Upregulated proteins in *panK*-integrated *S. peucetius* (BG200)

Spots that increased more than 1.5-fold in BG200 are presented in Table 1a and Fig. 4. Among the detected proteins, SP0864 and SP1972 are E1 and E3 components of

pyruvate dehydrogenase complex, respectively. Pyruvate dehydrogenase complex converts CoA into acetyl-CoA. SP0197 is an acetyl-CoA acetyltransferase that produces propionyl-CoA from 2-methyl-acetoacetyl-CoA, which is made from isoleucine through several biosynthetic steps. From these upregulated proteins and the malonyl-CoA quantification mentioned above, it was once again confirmed that integration of *E. coli panK* into *S. peucetius* increased the CoA pool, subsequently leading to enhanced acetyl-CoA, malonyl-CoA, and propionyl-CoA pools. SP1518 is a guanosine pentaphosphate synthetase known as a stringent response factor. Since the levels of highly phosphorylated guanosine nucleotides ppGpp and pppGpp synthesis often increase prior to onset of antibiotic production, the 2D gel data agree with the observation that *panK* integration increased the CoA pool as well as antibiotic production of *S. peucetius*.

Downregulated proteins in *panK*-integrated *S. peucetius* (BG200)

Spots that decreased more than 1.5-fold in BG200 are presented in Table 1b and Fig. 4. Fructose-bisphosphate aldolase SP6442, glyceraldehyde-3-phosphate dehydrogenase SP2164, and aconitase SP0177, which are involved in central carbon metabolism such as glycolysis and TCA cycle, are downregulated in BG200 gels. Huang et al. showed that major metabolic enzymes engaged in central metabolism were downregulated in their messenger RNA (mRNA) level during antibiotic production phase [6], suggesting that the enhanced CoA level changed cell metabolism to promote production of secondary metabolites. Likewise, oxidoreductase SP2018, thioredoxin reductase SP1774 (TrxB), and superoxide dismutase SP4049 (SodF) were also downregulated. Gram-positive

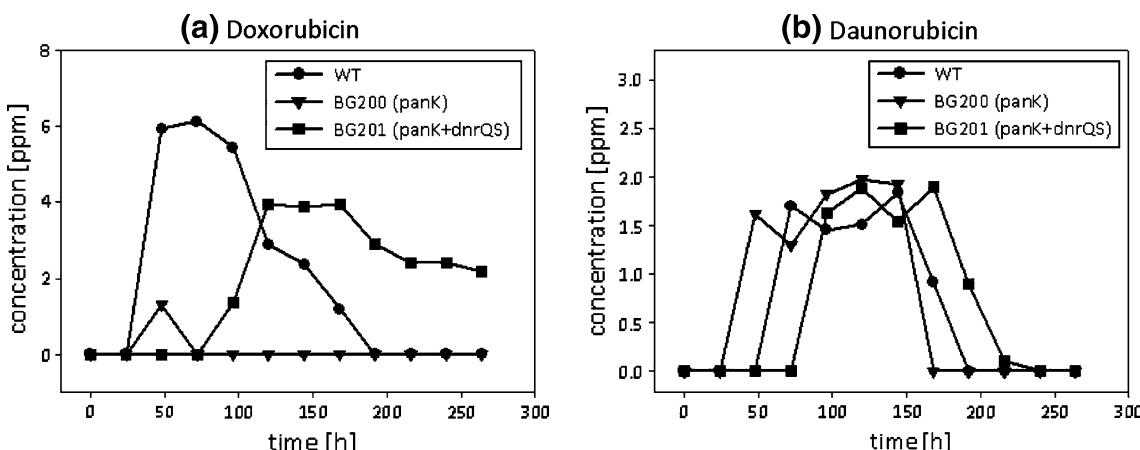
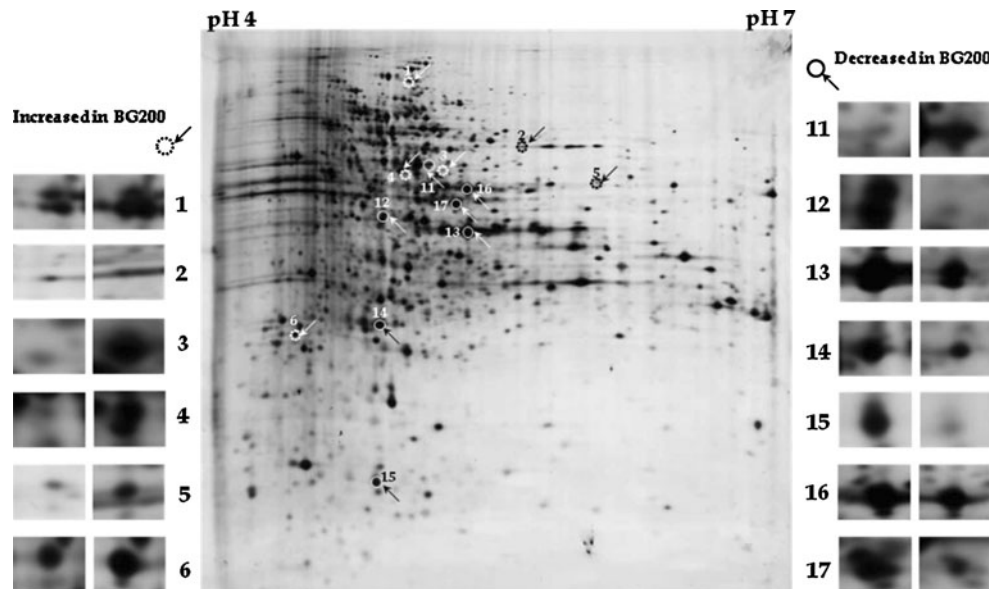


Fig. 3 Time course of doxorubicin (DXR) (a) and daunorubicin (DNR) (b) production of parental strain *S. peucetius* ATCC 27952 (filled circles), BG200 (*panK*-integrated *S. peucetius*) (filled inverted triangles), and BG201 (*dnrQS*-overexpressed *panK*-integrated *S. peucetius*) (filled squares)

triangles), and BG201 (*dnrQS*-overexpressed *panK*-integrated *S. peucetius*) (filled squares)

Table 1 Spots (a) increased and (b) decreased more than 1.5-fold in *panK*-integrated *S. peucetius* compared with the parental *S. peucetius* strain

Number	Increase (fold)	Protein ID	Annotation
(a) Increased			
1	2.3	SP1518	Putative guanosine pentaphosphate synthetase
2	3.1	SP1972	Putative dihydrolipoamide dehydrogenase (E3 component of pyruvate dehydrogenase complex)
3	12.0	SP0864	E1 alpha subunit from pyruvate dehydrogenase complex
4	2.4	SP0864	E1 alpha subunit from pyruvate dehydrogenase complex
5	5.8	SP0197	Acetyl-CoA acetyltransferase
6	2.2	SP5502	tRNA ligase
Number	Decrease (fold)	Protein ID	Annotation
(b) Decreased			
11	3.8	SP2018	Putative oxidoreductase
12	15.7	SP1774	Thioredoxin reductase
13	1.7	SP6442	Putative fructose 1,6-bisphosphate aldolase
		SP0902	ABC transporter ATP-binding component
14	2.1	SP4049	Superoxide dismutase
15	3.0	SP6684	Unknown
16	1.9	SP2164	Glyceraldehyde-3-phosphate dehydrogenase
		SP0177	Aconitase
		SP3733	Putative nucleotide methyltransferase
17	2.8	SP0392	Putative histidinol-phosphate aminotransferase

Fig. 4 Indications of spots increased or decreased by more than 1.5-fold on the 2D gel image of *S. peucetius*: spots 1–6, increased in BG200 (*panK*-integrated *S. peucetius*); spots 11–17, decreased in BG200

actinomycetes, including streptomycetes, produce several antioxidative compounds such as thioredoxin and mycothiol to cope with oxidative damage [3]. Superoxide dismutase catalyzes dismutation of superoxide into oxygen and hydrogen peroxide, so that, with other oxidoreductase (SP2018) and thioredoxin reductase (SP1774), it appears to play a role in antioxidative defense system in cells exposed to oxygen. It was surprising to see that proteins involved in

the antioxidative mechanism were downregulated, when the increased CoA pool would lead to increase secondary metabolism as seen from enhanced production of RHO. However, HPLC analysis clearly showed that, in BG200, enhanced level of RHO did not lead to increase in DXR production. Since cytotoxic DXR was reported to accumulate superoxide in cytosol [2], it is observed that enzymes related to antioxidative mechanism such as

superoxide dismutase, thioredoxin, and some oxidoreductase are overexpressed at high DXR production phase. Since BG200 showed less DXR production, it is conceivable that proteins involved in antioxidative process do not need to be highly expressed.

The most interesting result was the detection of downregulation of DrrA, a well-known ATP-binding cassette (ABC) transporter adenosine triphosphate (ATP)-binding component, suggesting that low level of this protein may lead to poor transport of DXR outside the cells and eventually transient increase in intracellular levels of DXR in BG200 strain, which might cause strong feedback inhibition of DXR synthesis, as shown in the HPLC analysis. Thus, it is conceivable that DXR production is tightly regulated by the transporter protein of corresponding antibiotics, determining their synthesis rate. To confirm this hypothesis, DXR/DNR resistance proteins were overexpressed in BG200.

Increased DXR production in *drrAB*-overexpressed *panK*-integrated *S. peucetius* (BG204)

DXR resistance system in *S. peucetius* comprises DrrA, B, and C. DrrA and DrrB together form an ATP-dependent efflux pump for transporting DXR and DNR outside the cell [5]. DrrA is a peripheral membrane protein that binds ATP in a DXR-dependent manner. DrrB forms a channel to export DXR and DNR [9]. DrrC provides self-resistance to the cell through excision repair of DNA by DXR and DNR. Since the stop codon of *drrA* overlaps with the start codon of *drrB*, they are translationally coupled [19].

The 2D gel electrophoresis data revealed downregulation of DrrA in *S. peucetius* BG200, as mentioned above. To overcome this problem, overexpression of *drrAB* was attempted. Expression plasmid pDrrAB25 [12] was

introduced into BG200 to construct *S. peucetius* BG204 strain. This strain produced twofold increase in DXR compared with the parental *S. peucetius* ATCC 27952 strain and 9.4-fold compared with BG200, suggesting that DrrAB was the rate-limiting step to synthesize more DXR in *panK*-integrated strain. Similarly, production of DNR was increased by 3.5-fold compared with the parental strain and 3.2-fold compared with BG200, whereas RHO production was decreased by twofold. In summary, BG204 enhanced both DXR and DNR production and prolonged DXR production periods compared with its parental strain (Fig. 5). The results showed that increased CoA pools can be used successfully to synthesize DXR through RHO and DNR, but only when high expression of resistance gene *drrAB* enhances active transport of DXR and DNR.

On the other hand, Malla et al. reported that DrrC-overexpressed *S. peucetius* produced higher DXR compared with DrrAB- or DrrABC-overexpressed *S. peucetius* [12]. Firstly, this result suggests that overexpressing biosynthetic enzymes or resistant systems one by one does not lead to increased antibiotic production. If overexpression of both DrrAB and DrrC increased productivity separately, then it is expected that DrrABC may have synergistic effect. However, DrrABC-overexpressed *S. peucetius* produced the same amount as DrrAB-overexpressed strain, indicating that it is not easy to observe the synergistic effect in DXR production by combining all the genes related to DXR biosynthesis [12].

Secondly, the same pDrrC25 (*drrC*-harboring pIBR25 under the control of strong *ermE** promoter) was incorporated into BG200 to test whether it produces more DXR than pDrrAB25-incorporated BG200 (BG204), since DrrC-overexpressed *S. peucetius* ATCC 27952 produced more DXR than DrrAB-overexpressed *S. peucetius* [12]. However, DrrC-overexpressed *panK*-integrated *S. peucetius*

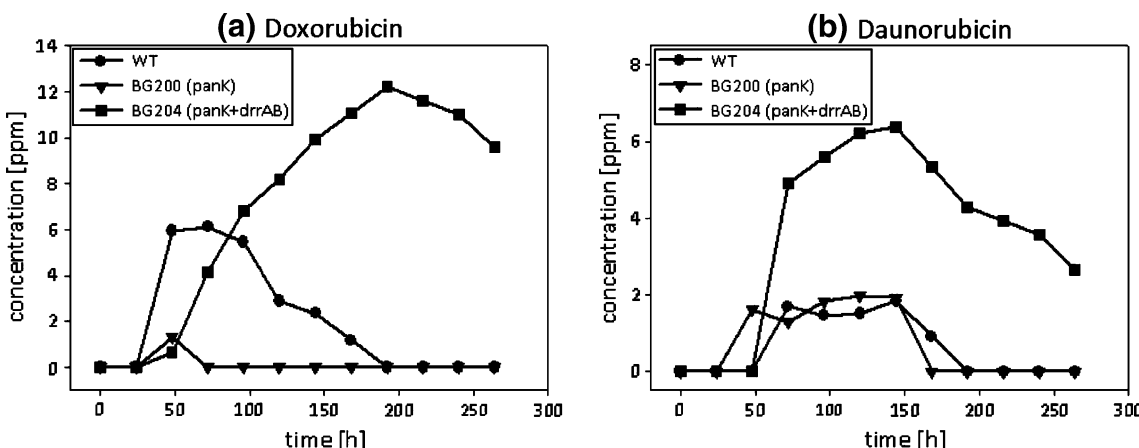


Fig. 5 Time course of doxorubicin (DXR) (a) and daunorubicin (DNR) (b) production of parental strain *S. peucetius* ATCC 27952 (filled circles), BG200 (*panK*-integrated *S. peucetius*) (filled inverted triangles), and BG204 (*drrAB*-overexpressed *panK*-integrated *S. peucetius*) (filled squares)

produced the same amount of DXR as the parental strain, indicating that DrrC did not enhance DXR production in BG200.

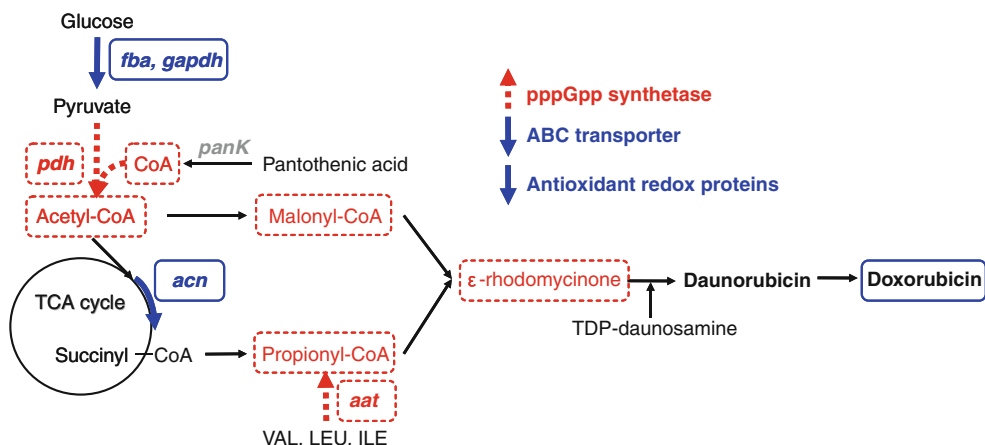


Fig. 6 Changes in the central metabolic pathway revealed by 2D gel, HPLC, and mass spectrometric analyses around the acetyl-CoA node, including the simplified doxorubicin (DXR) biosynthetic pathway. Upregulated reactions, proteins, and metabolites are indicated by dotted arrows and squares. Downregulated reactions, proteins, and

metabolites are indicated by thick solid arrows and squares. Abbreviations: fba, fructose 1,6-bisphosphate aldolase; gapdh, glyceraldehyde-3-phosphate dehydrogenase; pdh, pyruvate dehydrogenase complex; acn, aconitase; aat, acetyl-CoA acetyltransferase

produced less DXR compared with the parental strain *S. peucetius* ATCC 27952 (data not shown), indicating that the bottleneck in DXR production in the *panK*-integrated strain was efflux pump. This result strongly suggests that reverse-engineering is valuable in pointing out the major bottleneck among the important factors in biosynthesis of DXR or other useful compounds in a certain strain modified from wild type.

Conclusions

In this study, we showed that integration of *E. coli panK* gene into *S. peucetius* is functional in the cell, increasing the acyl-CoA pool and subsequently enhancing polyketide synthase (PKS)-type antibiotic production (Fig. 6). Here, *panK* integration increased CoA, acetyl-CoA, malonyl-CoA, and propionyl-CoA pools, which led to twofold increase in RHO production only. However, DNR production was not changed, and DXR production was rather decreased compared with the parental strain. Therefore, to enhance yields of DNR and DXR, glycosyltransferase (DnrS) and its helper protein (DnrQ) were overexpressed in *panK*-integrated *S. peucetius*. Although DXR production was increased threefold compared with BG200, almost the same and lower yields of DNR and DXR were obtained compared with WT. On the other hand, enhancing glycone production may lead to increased production of glycosylated DNR and DXR. So, we tried to increase glycone production by overexpressing two enzymes among the whole glycone biosynthetic cluster. However, this only produced similar amounts of DXR to WT (data not shown). Therefore, we reached the conclusion that the bottleneck in

DXR/DNR production in RHO-overproducing BG200 was neither glycosylation nor glycone biosynthesis efficiency. This result strongly indicates that simple addition of biosynthetic enzymes to increase antibiotic production does not always work, because *Streptomyces* has complex regulatory mechanism for cell differentiation and secondary metabolite production.

To elucidate the main reason for the intermediate metabolite accumulation, comparative 2D gel analysis was performed to understand the global changes in BG200 and to investigate the main cause of this low product yield. Results of 2D gel analysis of BG200 and *S. peucetius* ATCC 27952 indicated that BG200 showed the representative phenotype of stationary-phase cell metabolism and produced more overall anthracycline polyketide shown as downregulated proteins that are involved in central metabolism and upregulated pentaphosphate synthetase. Among the downregulated proteins in BG200, DrrA which forms ATP-dependent efflux pump for DXR and DNR, was detected. Based on this observation, DrrAB-overexpressed BG200 (BG204) was constructed. In BG204, DXR production level was increased twofold and 9.4-fold compared with *S. peucetius* ATCC 27952 and BG200, respectively. This result finally demonstrated that 2D gel proteomic analysis and metabolite quantification in parallel gave key clues to understand the effect of *panK* integration into parental *S. peucetius* ATCC 27952 on DXR production. This gave comprehensive explanations for global proteomic changes in BG200 and provided a clue for successfully increasing DXR production. In conclusion, *panK* integration alone does not work properly, so the transporter protein of DXR should be coexpressed to increase DXR production.

Acknowledgments This work was supported by WCU program (R322009000102130), Basic Science Research Program (2010-0009942), Priority Research Centers Program (2009-0094021), and NRL Program (20090083035) through the National Research Foundation (NRF) grant funded by the Korea Government (MEST).

References

- Dekleva ML, Titus JA, Strohl WR (1985) Nutrient effects on anthracycline production by *Streptomyces peucetius* in a defined medium. *Can J Microbiol* 31:287–294
- den Hartog GJ, Haenen GR, Vegter E, van der Vijgh WJ, Bast A (2003) Superoxide dismutase: the balance between prevention and induction of oxidative damage. *Chem Biol Interact* 145:33–39
- Fahey RC (2001) Novel thiols of prokaryotes. *Annu Rev Microbiol* 55:333–356
- Flett F, Mersinias V, Smith CP (1997) High efficiency intergenic conjugal transfer of plasmid DNA from *Escherichia coli* to methyl DNA-restricting streptomycetes. *FEMS Microbiol Lett* 155:223–229
- Guilfoile PG, Hutchinson CR (1991) A bacterial analog of the mdr gene of mammalian tumor cells is present in *Streptomyces peucetius*, the producer of daunorubicin and doxorubicin. *Proc Natl Acad Sci U S A* 88:8553–8557
- Huang J, Lih CJ, Pan KH, Cohen SN (2001) Global analysis of growth phase responsive gene expression and regulation of antibiotic biosynthetic pathways in *Streptomyces coelicolor* using DNA microarrays. *Genes Dev* 15:3183–3192
- Hutchinson CR, Colombo AL (1999) Genetic engineering of doxorubicin production in *Streptomyces peucetius*: a review. *J Ind Microbiol Biotechnol* 23:647–652
- Jackowski S, Rock CO (1981) Regulation of coenzyme a biosynthesis. *J Bacteriol* 148:926–932
- Kaur P (1997) Expression and characterization of DrrA and DrrB proteins of *Streptomyces peucetius* in *Escherichia coli*: DrrA is an ATP binding protein. *J Bacteriol* 179:569–575
- Kieser T, Bibb MJ, Buttner MJ, Chater K, Hopwood DA (2000) Practical *Streptomyces* genetics: John Innes Centre, Norwich Research Park, Colney, Norwich, UK
- Malla S, Niraula NP, Liou K, Sohng JK (2009) Enhancement of doxorubicin production by expression of structural sugar biosynthesis and glycosyltransferase genes in *Streptomyces peucetius*. *J Biosci Bioeng* 108:92–98
- Malla S, Niraula NP, Liou K, Sohng JK (2009) Self-resistance mechanism in *Streptomyces peucetius*: Overexpression of drrA, drrB and drrC for doxorubicin enhancement. *Microbiol Res* 165(4):259–267
- Massoni A, Moes S, Perrot M, Jenoe P, Boucherie H (2009) Exploring the dynamics of the yeast proteome by means of 2-DE. *Proteomics* 9(20):4674–4685
- Moore BS, Hertweck C (2002) Biosynthesis and attachment of novel bacterial polyketide synthase starter units. *Nat Prod Rep* 19:70–99
- Noh JH, Kim SH, Lee HN, Lee SY, Kim ES (2010) Isolation and genetic manipulation of the antibiotic down-regulatory gene, wbla ortholog for doxorubicin-producing *Streptomyces* strain improvement. *Appl Microbiol Biotechnol* 86(4):1145–1153
- Olano C, Lomovskaya N, Fonstein L, Roll JT, Hutchinson CR (1999) A two-plasmid system for the glycosylation of polyketide antibiotics: bioconversion of epsilon-rhodomycinone to rhodomycin D. *Chem Biol* 6:845–855
- Otten SL, Liu X, Ferguson J, Hutchinson CR (1995) Cloning, characterization of the *Streptomyces peucetius* dnrQS genes encoding a daunosamine biosynthesis enzyme, a glycosyltransferase involved in daunorubicin biosynthesis. *J Bacteriol* 177:6688–6692
- Park JW, Jung WS, Park SR, Park BC, Yoon YJ (2007) Analysis of intracellular short organic acid-coenzyme a esters from actinomycetes using liquid chromatography-electrospray ionization-mass spectrometry. *J Mass Spectrom* 42(9):1136–1147
- Pradhan P, Li W, Kaur P (2009) Translational coupling controls expression and function of the DrrAB drug efflux pump. *J Mol Biol* 385:831–842
- Sthapit B, Oh TJ, Lamichhane R, Liou K, Lee HC, Kim CG, Sohng JK (2004) Neocarzinostatin naphthoate synthase: an unique iterative type I PKS from neocarzinostatin producer *Streptomyces carzinostaticus*. *FEBS Lett* 566:201–206
- Vadali RV, Bennett GN, San KY (2004) Enhanced isoamyl acetate production upon manipulation of the acetyl-CoA node in *Escherichia coli*. *Biotechnol Prog* 20:692–697
- Vadali RV, Bennett GN, San KY (2004) Cofactor engineering of intracellular CoA/acetyl-CoA and its effect on metabolic flux redistribution in *Escherichia coli*. *Metab Eng* 6:133–139
- Vadali RV, Bennett GN, San KY (2004) Applicability of CoA/acetyl-CoA manipulation system to enhance isoamyl acetate production in *Escherichia coli*. *Metab Eng* 6:294–299
- Vallari DS, Jackowski S (1988) Biosynthesis and degradation both contribute to the regulation of coenzyme A content in *Escherichia coli*. *J Bacteriol* 170:3961–3966
- Yates JR 3rd (2004) Mass spectral analysis in proteomics. *Annu Rev Biophys Biomol Struct* 33:297–316